UC Berkeley
UC Berkeley Previously Published Works

Title

High throughput, spatially resolved thermal properties measurement using attachable and reusable 3ω sensors

Permalink

https://escholarship.org/uc/item/57v6x59g

Journal

Review of Scientific Instruments, 94(9)

ISSN

0034-6748

Authors

Chalise, Divya
Tee, Richard
Zeng, Yuqiang
et al.

Publication Date

2023-09-01

DOI

10.1063/5.0151160

Peer reviewed

eScholarship.org Powered by the California Digital Library
University of California

Review of Scientific Instruments

RESEARCH ARTICLE | SEPTEMBER 07 2023

High throughput, spatially resolved thermal properties measurement using attachable and reusable 3ω sensors

Divya Chalise ; Richard Tee ; Yuqiang Zeng; Sumanjeet Kaur ; Himanshu Pokharna ;
Ravi S. Prasher

Rev. Sci. Instrum. 94, 094901 (2023)
https://doi.org/10.1063/5.0151160

View Online
Export Citation
CrossMark

09 February 2024 17:58:44

Review of Scientific Instruments | ARTICLE | pubs.aip.org/aip/rsi

High throughput, spatially resolved thermal properties measurement using attachable and reusable 3ω sensors

Cite as: Rev. Sci. Instrum. 94, 094901 (2023); doi: 10.1063/5.0151160
Submitted: 19 March 2023 • Accepted: 17 August 2023 •
Published Online: 7 September 2023

View Online

Export Citation

CrossMark

Divya Chalise,[1,2] Richard Tee,[1,2] Yuqiang Zeng,[2] Sumanjeet Kaur,[2] Himanshu Pokharna,[3] and Ravi S. Prasher[1,2,a)]

AFFILIATIONS

[1] Department of Mechanical Engineering, University of California, Berkeley, California 94720, USA
[2] Energy Technologies Area, Lawrence Berkeley National Lab, 1 Cyclotron Road, Berkeley, California 94720, USA
[3] Deeia Inc., Saratoga, California 95070, USA

[a)] **Author to whom correspondence should be addressed:** rsprasher@lbl.gov

ABSTRACT

The 3ω method is a well-established thermal technique used to measure the thermal conductivity of materials and the thermal resistance of interfaces. It has significant advantages over other steady state and transient thermal techniques in its ability to provide spatially resolved thermal property measurements over a wide range of thermal conductivity. Despite its advantages, it has been restricted to lab-scale use because of the difficulty involved in sample preparation and sensor fabrication and is limited to non-metallic substrates. High-throughput 3ω measurements with reusable sensors have not been realized yet. In this work, we demonstrate a method of applying reusable 3ω sensors fabricated on flexible polyimide films to measure bulk and spatially resolved thermal properties. We establish the limits of thermal conductivity measurement with the method to be 1 to 200 W/mK, and within the measurement limit, we verify the method by comparing the measured thermal conductivities of standard samples with established values. From the 3ω measurements, we also determine the thermal resistance of an interlayer of thermal grease as a function of pressure and compare it against the resistance calculated from direct thickness measurements to demonstrate the ability of this method to provide spatially resolved subsurface information. The technique presented is general and applicable to both metallic and non-metallic substrates, providing a method for high-throughput 3ω measurements with reusable sensors and without considerable sample preparation.

Published under an exclusive license by AIP Publishing. https://doi.org/10.1063/5.0151160

09 February 2024 17:58:44

INTRODUCTION

The 3ω method is a well-established frequency-domain thermal property measurement technique[1–4] that has been used to measure the thermal conductivity of bulk materials[1,5] and thin films[2,3,6] and the thermal resistance of interfaces.[4] This method has also been modified for non-conventional uses such as gas sensing[7] and fouling thickness measurement.[8] Recently, 3ω sensors embedded in batteries have been used to measure lithium distribution in electrodes[9] and lithium deposition morphology at the lithium metal-solid state electrolyte interface.[10]

The 3ω method has numerous advantages compared to traditional methods for thermal conductivity measurement. Steady state thermal conductivity measurement methods, such as the cut-bar method[4,11] and the heat flow meter-based methods,[12,13] measure the overall thermal resistance of the sample and the interfaces between the sample and the sensors. The interface resistance is assumed to be constant across multiple measurements, and the total thermal resistance of samples of different thicknesses is used to extract the thermal conductivity of the sample. If the sample thermal resistance is small compared to the interface thermal resistance, a small discrepancy in the interface resistance across the measurements can lead to a significant error in the extracted thermal conductivity. Unlike the steady state methods, the 3ω method is a frequency domain technique with a frequency dependent thermal penetration depth,[3] which allows spatially resolved thermal measurement of multiple layers and interfaces beneath the sensor. This spatial resolution allows the decoupling of the interface resistance

Published under an exclusive license by AIP Publishing

between the sensor and the substrate from the thermal properties of the substrate, allowing independent thermal interface resistance and thermal conductivity measurements without ambiguity. Unlike other transient methods such as a transient planar source (TPS)[14] and the laser-flash method (LFM),[15] which are limited to bulk samples, and time-domain thermoreflectance (TDTR),[16] which is limited to thin films and/or high thermal conductivity samples, the 3ω method can measure a wide range of thermal conductivity[17] across samples of various dimensions (from a few micrometers to bulk). Furthermore, by varying the sensor geometry, the 3ω measurements can be made selectively sensitive to in-plane or cross-plane thermal conductivity,[3,6] allowing independent measurement of the anisotropic thermal conductivity tensor in anisotropic samples.

Despite the numerous advantages, high-throughput spatially resolved 3ω measurements with reusable sensors have not been realized, and wide-scale adoption of the 3ω method has been severely limited. Traditionally, 3ω sensors are deposited on the samples. This requires the sample surface to be nominally planar with an average roughness of the order of less than a micrometer, as the sensor thickness is of the order of 100 nanometers.[4,9] Moreover, the sensors deposited on one sample cannot be reused on other samples. Even though earlier work[18] has reported reusable and attachable 3ω sensors, the thermal interface resistance between the sample and the sensor in those experiments was rather large, and since this thermal interface resistance dominates the 3ω signal, the method reported is not sensitive enough for spatially resolved thermal measurements or high thermal conductivity measurements. Therefore, the measurements are limited to low thermal conductivity samples (e.g., human skin, as presented in the work). Further, in metallic substrates, an additional dielectric layer needs to be deposited between the sensor and the metallic substrate to electrically isolate the sensor from the metal substrate, requiring an additional step in sample preparation for 3ω measurements.

In this work, we report a method of employing reusable 3ω sensors fabricated on polyimide (Kapton®) films for high-throughput thermal measurements. We use a high thermal conductivity (k) thermal paste under a considerable (30 psi) external pressure to act as an intermediate layer between the sensor and the sample to minimize the interfacial thermal resistance and allow high thermal conductivity measurements. The same thermal paste acts as a dielectric film to isolate the sensor from metallic substrates, allowing 3ω measurement of metallic samples without any additional surface modification. This method eliminates the shortcomings of the general 3ω method discussed earlier, thereby enabling the potential for wide-scale application of the 3ω method for high-throughput thermal measurements.

METHODS

Sensor design, fabrication and 3ω instrumentation

3ω sensors were fabricated on 25 μm polyimide (Kapton®) film by depositing 100 nm gold with a 10 nm chromium adhesion layer (e-beam evaporation) through a custom shadow mask. Two sensors [shown in Fig. 1(a)] with different sensor lengths and half-widths were fabricated on the same film to allow measuring different sample sizes. The outer sensor was 9 mm long and 300 μm wide, while the inner sensor was 6 mm long and 200 μm wide. The connection pads for electrical connections to each sensor were fabricated away from the sensor to allow for the application of high pressure on the sensor/sample stack without breaking the electrical connections. Insulated copper wires were connected to the connection pads using EPO-TEK®H20E silver-infused epoxy. The temperature coefficient of resistance (TCR) was calibrated for each sensor by measuring the 4-point resistance with an Agilent 34401A digital multimeter at temperatures between 25 and 40 °C. The 3ω voltage across the sensor was measured using a Stanford Research Systems SR830 lock-in amplifier, and the 1ω AC current passing through the sensor was supplied using a Keithley 6221 current source. Additionally, a custom circuit was employed to cancel the 1ω voltage originating from the sensor resistance.

Measurement procedure

X23-7783D thermal paste from MicroSi was applied at ~30 psi stack pressure between the sample and the 3ω sensor fabricated on the polyimide film to minimize the contact resistance between the

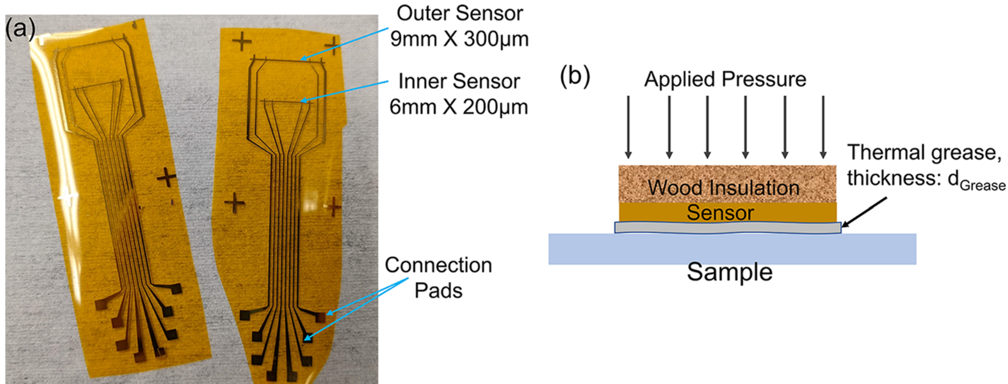

FIG. 1. (a) 3ω sensors fabricated on polyimide film. Each set contains two sensors, one inner and one outer, to allow for the measurement of samples of different sizes. The connection pads are fabricated away from the sensor to enable the application of high pressure on the sample/sensor stack. (b) A typical measurement stack with the sensor and the thermal grease sandwiched between the sample and a rigid insulation layer (typically wood) at high external pressure.

09 February 2024 17:58:44

Published under an exclusive license by AIP Publishing

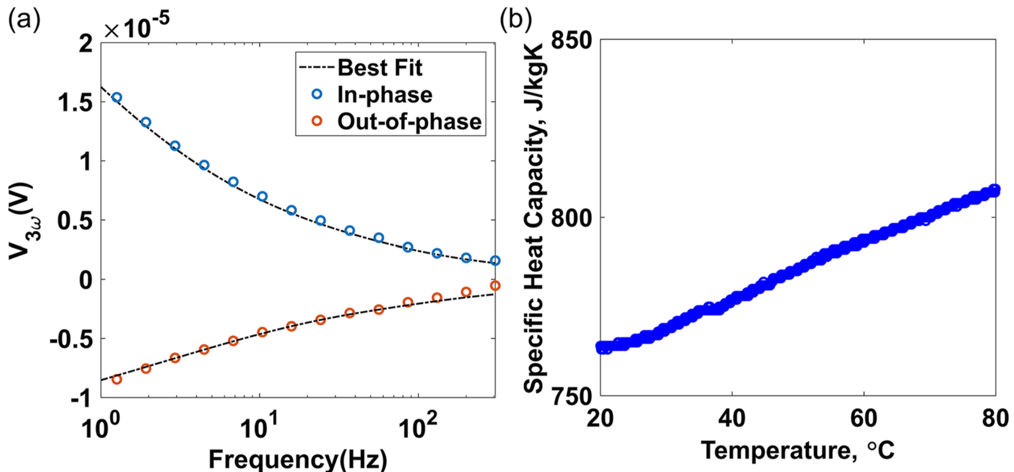

FIG. 2. (a) 3ω fits to determine the thermal conductivity of the thermal paste. From the measurement, the thermal conductivity was determined to be 7 W/mK. (b) Specific heat capacity of the thermal paste plotted as a function of temperature measured using differential scanning calorimetry (DSC). The room temperature (25 °C) specific heat capacity of the thermal grease is 770 J/kgK.

sensor and the sample. First, ~250 to 350 mg of thermal grease were applied to the sample to ensure full coverage of the thermal paste over an area of more than 1 in^2. Then the 3ω heater line was stacked on top of the grease, and a 1in^2 wooden insulation block was stacked on top of the 3ω sensor, forming a stack of insulation, a 3ω sensor on polyimide, thermal grease, and the sample [shown in Fig. 1(b)]. The thermal conductivity of the wooden insulation was assumed to be 0.2 W/mK for all the measurements but varied between 0.1 and 0.4 W/mK for uncertainty calculations. Using a pressure clamp, ~30 lbs. of pressure was applied to the stack to ensure contact and thinning of the thermal grease layer to about 30–50 μm. While doing so, it was ensured that there was no tilt of the wood insulation, which could affect the uniformity of the grease thickness. The 3ω measurement was performed using a custom LabVIEW program with the instrumentation described earlier. For each frequency in the 3ω measurement, the demodulated signal from the lock-in amplifier was sampled at a sampling rate of 4 Hz and was averaged for a sampling time of 60 s. All the 3ω measurements were performed in the frequency range of 0.1–310 Hz.

Paste thermal characterization

The specific heat capacity of the thermal interface paste was measured by differential scanning calorimetry (DSC) using the TA Instruments Discovery DSC 2500 by direct heat flow measurement calibrated against a sapphire reference. The temperature was equilibrated at 10 °C for 5 min and ramped to 80 °C at 10 °C/min. The specific heat capacity measured as a function of temperature is presented in Fig. 2(b). The average specific heat capacity at room temperature was determined to be 770 J/kgK. The density measurement was done from mass and volume measurements, rendering

09 February 2024 17:58:44

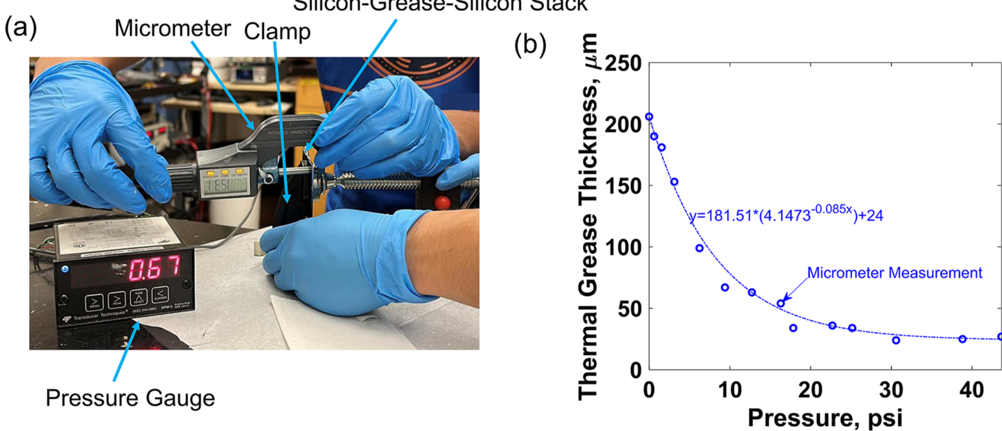

FIG. 3. (a) Experimental setup to characterize the thickness of the paste as a function of stack pressure. The thickness measurement is done using a micrometer on a stack of thermal grease sandwiched between silicon plates. The pressure is varied using a clamp and monitored with a calibrated piezoelectric pressure gauge. (b) The paste thickness plotted as a function of pressure in psi. The circles represent the experimental measurement, and the dotted-line is an empirical exponential best-fit.

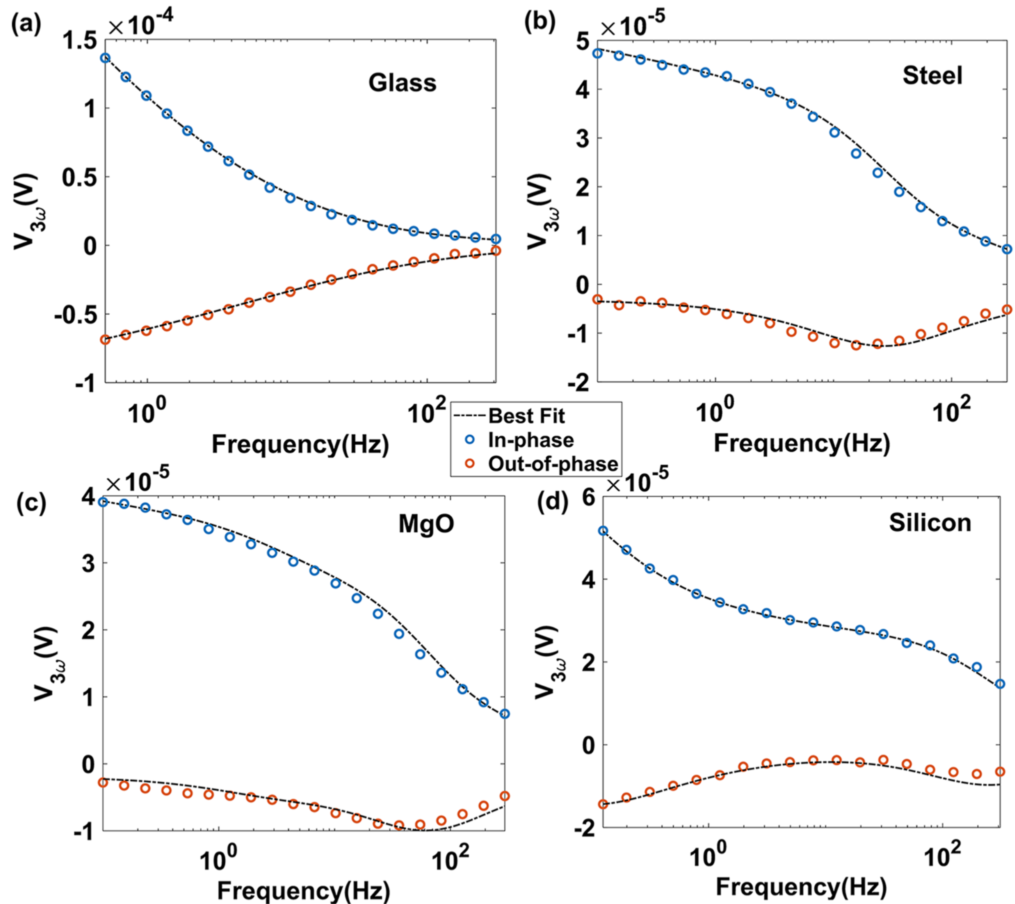

FIG. 4. 3ω measurements along (circles) with the best-fit lines (dashes) to determine the thermal conductivities of glass (a), sapphire (b), MgO (c), and steel (d), respectively. The high frequency signal (~10 to 300 Hz) with a shorter penetration depth is used to fit the thickness of the paste, whereas the low frequency signal (<10 Hz) is used to fit the sample thermal conductivity.

the room temperature volumetric heat capacity to be 1.87 MJ/m^3K. The thermal conductivity of the paste was determined using the 3ω method. A 3ω sensor was deposited on a glass slide of known thermal conductivity, and the thermal paste was squeezed at 30 psi pressure between two glass slides with the sensor on one of them. The 3ω measurement was carried out between 1 and 310 Hz. From the best-fit to the 3ω data [shown in Fig. 2(a)], the thermal conductivity of the thermal paste at room temperature was determined to be 7 W/mK.

Thermal paste thickness measurement

To characterize the thickness of the thermal paste as a function of stack pressure, the high thermal conductivity paste was sandwiched between two silicon wafers of known thickness and a 1×1 in^2 cross section. The pressure of the sandwiched stack was varied by a clamp and measured using a calibrated piezoelectric pressure-sensor described in our earlier work.[10] The thickness was measured by a digital micrometer with a resolution of 1 μm to quantify the thickness of the paste as a function of stack pressure. The measurement setup is presented in Fig. 3(a), and the measured thickness as a function of the stack pressure along with the best-fit curve is presented in Fig. 4(b).

RESULTS

Standard thermal conductivity measurements

The thermal conductivity measurements of standard materials with a range of thermal conductivities were conducted to validate the measurement method and establish an upper limit for the thermal conductivity measurement. We measured the thermal conductivities of fused silica, magnesium oxide (MgO), steel (ASTM A108, 0.5% carbon), and doped silicon with the proposed method and compared them against thermal conductivities obtained from standard 3ω measurement with sensors deposited on the sample (except steel , whose standard thermal conductivity was obtained from the literature (Ref. 21)[20,19]). The 3ω fits for the standard measurements are shown in Fig. 4. From the best fit, the obtained thermal conductivities are presented in Table I along with the standard thermal conductivities.

09 February 2024 17:58:44

Published under an exclusive license by AIP Publishing

The measurement sensitivity (S_p) to a measurement parameter "p" is the percentage change in the signal for a percentage change in the parameter. It can be defined as $S_p = \frac{dln(V_{3\omega})}{dln(p)} = \frac{p}{V_{3\omega}}\frac{dV_{3\omega}}{dp}$, where $V_{3\omega}$ is the magnitude of the 3ω voltage measured. The 3ω fit and the respective measurement sensitivities for the standard sample measurements are presented in Fig. 4. For glass, the sample thermal conductivity is lower than the grease thermal conductivity; therefore, the measurement is not sensitive to the thermal paste thickness at all frequencies and is selectively sensitive to the glass thermal conductivity. For other samples whose thermal conductivity is greater than that of the thermal paste, at high frequencies (10–300 Hz), the 3ω measurement is selectively sensitive to the thermal properties of the thermal paste. With the thermal conductivity and the heat capacity of the thermal paste known, we fit the paste thickness to match the 3ω signal (both in-phase and out-of-phase) at high frequencies. At lower frequencies (~0.1 to 10 Hz), the 3ω measurement is sensitive to the sample thermal conductivity. With the paste thickness obtained from the high-frequency fit, the sample thermal conductivity is then obtained from the lower frequency 3ω fit (Fig. 5).

Even if small, the thermal paste presents an interfacial resistance that negatively affects the measurement sensitivity for high conductivity samples. Therefore, there is a need to establish the

TABLE I. Comparison of the measured and standard thermal conductivities of samples.

Material	Measured thermal conductivity (W/mK)	Standard thermal conductivity (W/mK)
Glass	1.09 ± 0.15	1.18[a]
MgO	45.8 ± 2.0	50[a]
Steel (ASTM A108, 0.5% carbon)	42.6 ± 3.5	40[19]
p-doped silicon	122.03 ± 4.7	120[a]

[a]Measured using the standard 3ω method with the sensor deposited on the sample.

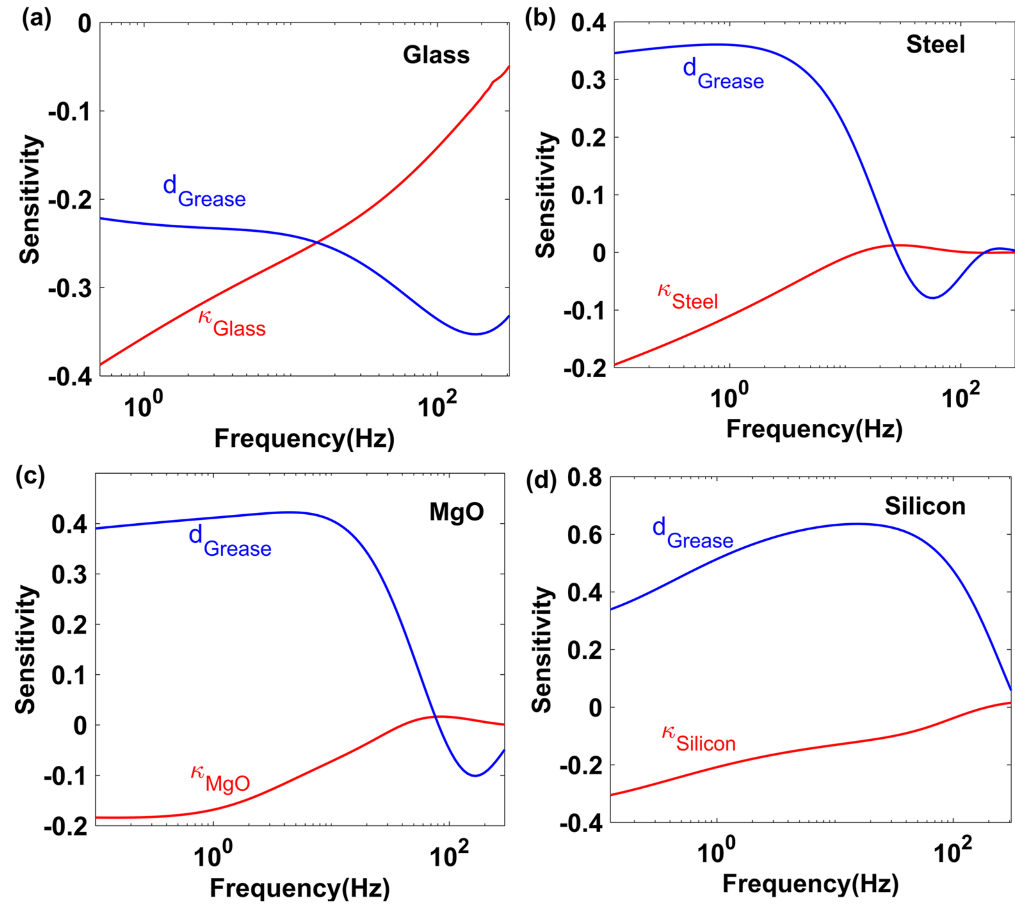

FIG. 5. Plots showing measurement sensitivity as a function of frequency for the two fitting parameters (paste thickness and sample thermal conductivity) for glass (a), steel (b), MgO (c), and p-doped silicon (d). The high frequency signal (10–300 Hz) is exclusively sensitive to the paste thickness and is, therefore, used for obtaining the paste thickness. At lower frequencies (0.1 to 10 Hz), the measurement is sensitive to the sample's thermal conductivity and can, therefore, be used to extract the sample thermal conductivity.

09 February 2024 17:58:44

Published under an exclusive license by AIP Publishing

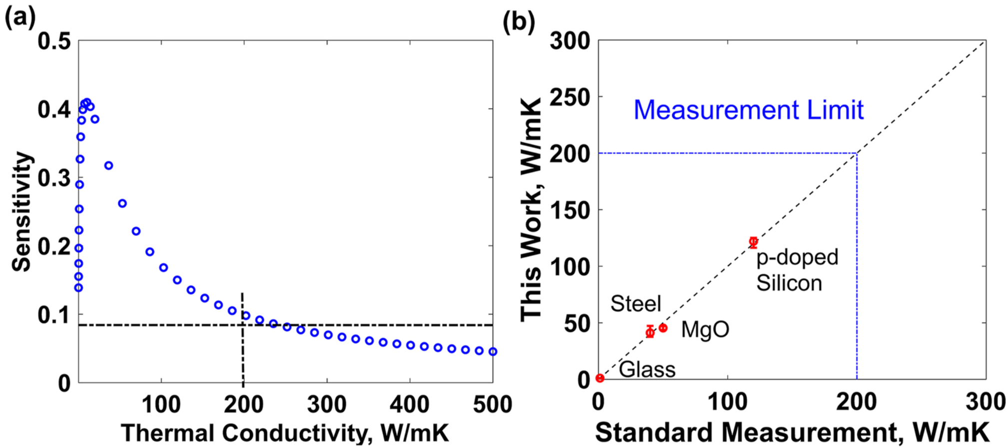

FIG. 6. (a) Maximum measurement sensitivity to the sample thermal conductivity plotted as a function of the sample thermal conductivity. For samples with very low thermal conductivity, the heat loss to the insulation layer becomes significant, and the measurement sensitivity is compromised. The optimal measurement sensitivity is obtained for a sample thermal conductivity of ~5 W/mK, after which the measurement sensitivity decreases monotonically as the grease thermal resistance becomes dominant. For reliable measurements, we set the cutoff sensitivity to 0.1, corresponding to the sample thermal conductivity of 200 W/mK, which is the measurement limit with this method. (b) Comparison of the thermal conductivity measured from standard methods to the thermal conductivity measured using the approach described in this work. Within the measurement limit, the obtained thermal conductivities agree well with the standard measurements.

upper limit of thermal conductivity measurement with the proposed method. To do so, we set the thickness of the thermal paste to 50 μm and varied the sample thermal conductivity to determine the maximum sensitivity of the sample thermal conductivity within the frequency range of 100 mHz to 310 Hz. Within the frequency range, the maximum sensitivity as a function of the sample thermal conductivity is presented in Fig. 6(a). When the sample thermal conductivity is small and comparable to that of the wooden insulation layer on top of the sensor (~0.2 W/mK), the heat loss to the insulation layer becomes important, and the measurement sensitivity is compromised. Therefore, we consider 1 W/mK as the lower limit of the thermal conductivity measurement using this method. As the thermal conductivity increases, the absolute measurement sensitivity increases and reaches its maximum when the sample thermal conductivity is ~5 W/mK. Beyond that, the sensitivity decreases monotonically since the thermal paste resistance becomes dominant as the sample thermal resistance decreases. We choose a sensitivity of 0.1 to be the cut-off sensitivity for reasonable measurement accuracy as the 3ω measurement resolution for typical 3ω voltages (of the order of 10 s of μV) is only accurate

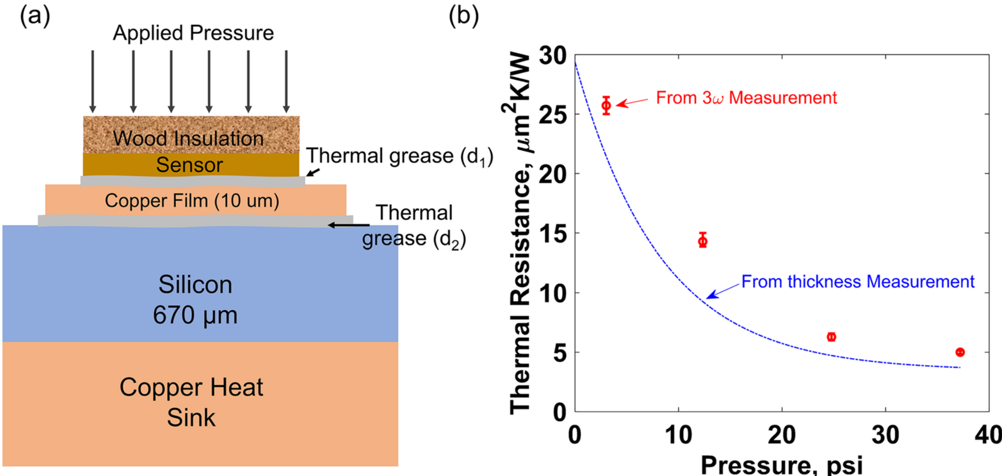

FIG. 7. (a) Setup to measure the thermal resistance of the interlayer thermal grease from 3ω measurements using the attachable sensor. The thermal grease is sandwiched between a 10 μm copper film and a 670 μm thick silicon wafer. The same setup with the sensor and thermal grease with a rigid insulation layer on top is used to perform the 3ω measurements. (b) The interlayer thermal resistance measured from the 3ω method compared to the thermal resistance calculated from the grease thickness obtained from the micrometer measurement. The thermal resistance obtained from the 3ω measurements is within the range of that obtained from the micrometer measurements, and the qualitative trend of the monotonic decrease below 30 psi and saturation above 30 psi is evident.

09 February 2024 17:58:44

Published under an exclusive license by AIP Publishing

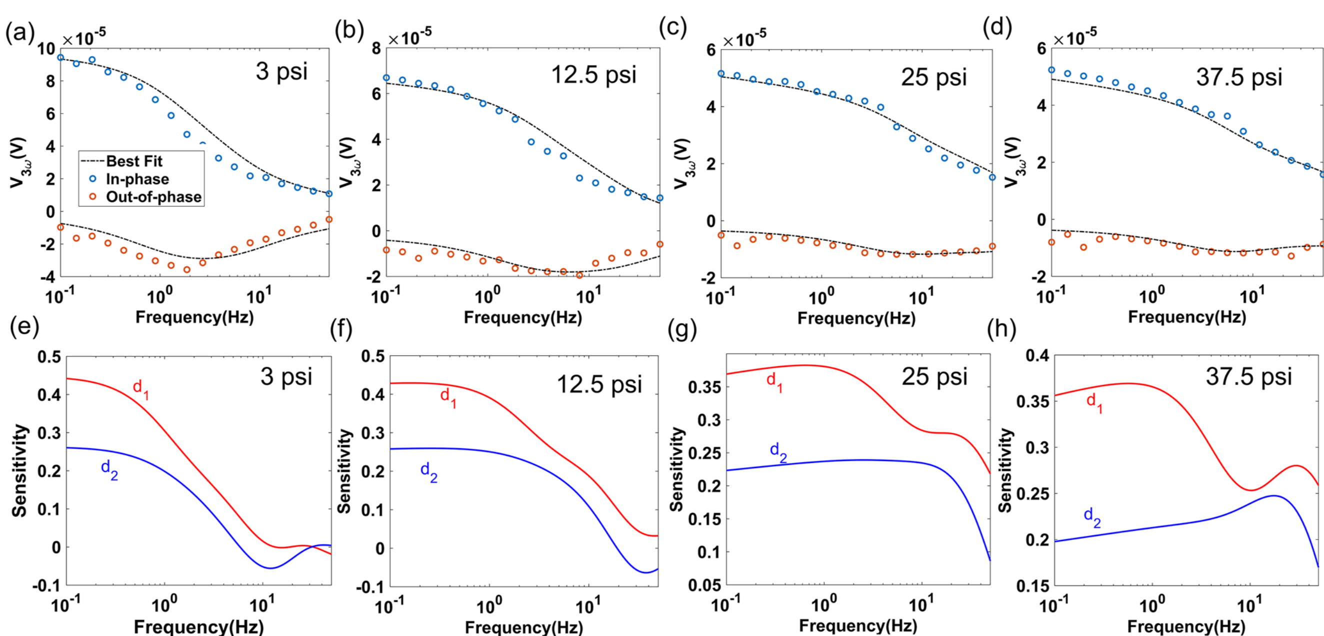

FIG. 8. 3ω measurements (circles) along with the best fit (dashed) curves to extract the interlayer thickness (d_2) at (a) 3 psi, (b) 12.5 psi, (c) 25 psi, and (d) 37.5 psi stack pressure. (e)–(h) are the respective measurement sensitivities to the thickness (d_1) of the thermal paste between the stack and the sensor and the interlayer thickness (d_2) between copper and silicon. As the stack pressure increases, the paste thickness (d_1) and the sensitivity to the first layer of the thermal paste decrease, and the measurement sensitivity to the second layer of the thermal paste (d_2) increases.

09 February 2024 17:58:44

enough to differentiate a 10% change in the signal (typically of the order of 1 μV). Below the cut-off sensitivity, a slight discrepancy in paste thermal resistance estimation can create a significant error in the measurement of the sample thermal conductivity. In Fig. 6(a), the thermal conductivity corresponding to the maximum measurement sensitivity of 0.1 (or 10%) is ~200 W/mK. Therefore, we estimate the maximum thermal conductivity measurement limit to be 200 W/mK for bulk thermal conductivity measurement using the proposed method. Figure 6(b) summarizes the comparison of the standard bulk thermal conductivity measurements to the measurements using the proposed method, along with the measurement limit (200 W/mK). In the figure, it is evident that our proposed method can accurately measure the thermal conductivity of bulk samples within the measurement limit.

Buried interlayer thickness measurement

One of the advantages of the 3ω method compared to transient time-domain methods such as TPS or LFM is that the 3ω method can provide spatially resolved thermal information, which can be used to extract subsurface properties. To test the effectiveness of the proposed technique to extract subsurface information from the 3ω measurements, we created a silicon–copper stack [Fig. 7(a)] with an interlayer of the thermal paste to extract the thermal resistance of the interlayer thermal paste at different stack pressures from the 3ω measurements. We chose the same thermal paste used at the sensor-sample interface since the paste thickness is well characterized from the micrometer-based measurement and can be used to directly verify the per unit area thermal resistance calculated from the thickness and thermal conductivity (7 W/mK) using the equation $R_{\text{int}} = d_{\text{int}}/\kappa_{\text{int}}$, where R_{int} is the thermal resistance of the interlayer, d_{int} is the interlayer thickness, and κ_{int} is the interlayer thermal conductivity. This resistance can be directly compared to that extracted from the 3ω method. Because the thermal properties of copper and silicon are known, we fit the thickness of the thermal paste (d_2) between copper and the sensor and between silicon and copper to extract the buried interlayer thermal resistance, assuming a known thermal conductivity of 7 W/mK for the thermal paste. Figures 8(a)–8(d) present the 3ω fits, and Figs. 8(e)–8(h) present the respective measurement sensitivities for the interlayer thickness measurements at 3, 12.5, 25, and 37.5 psi, respectively. As the stack pressure increases, the paste thickness as well as the sensitivity to the first layer of the thermal paste decrease, because of which the measurement sensitivity to the second layer of the thermal paste, i.e., the interlayer thickness, increases. Figure 7(b) compares the interlayer thermal resistance extracted from the 3ω measurement to the thermal resistance calculated from the thermal conductivity and the best-fit thickness measurement. The thermal resistance measured using the 3ω method is slightly higher but within the range of the thermal resistance calculated from the grease thickness measured using the micrometer. An offset between the 3ω measurement and the micrometer measurement can be seen, which we believe is caused by uneven pressing of the thermal grease between the copper foil and the silicon wafer, as compared to when pressed between two rigid silicon wafers in the case of the micrometer measurements. Nonetheless, the monotonic decrease in the thermal resistance as well as the saturation of the resistance beyond 30 psi pressure is well captured by the 3ω measurement.

Published under an exclusive license by AIP Publishing

DISCUSSION AND CONCLUSIONS

In this work, we have introduced a method of employing reusable 3ω sensors to bridge significant gaps in the adoption of the 3ω method for high-throughput thermal measurements. By applying a high thermal conductivity paste at a high external pressure to minimize the thermal resistance between the sensors, the proposed method allows the possibility of spatially resolved high thermal conductivity measurements previously not possible with attachable 3ω sensors. As the thermal paste acts as a dielectric layer between the sensor and the sample, the same method can be used for metallic samples without any modifications. In this work, we establish the upper limit of thermal conductivity measurement with the proposed method and show that within the established limit, the thermal conductivity measurements using this method are accurate compared to standard measurements. We also show that the proposed method is sensitive enough to perform spatially resolved 3ω measurements by extracting the thickness of interlayer thermal paste entirely from 3ω measurements. Even though the experiments presented here use only one type of commercial high conductivity thermal paste, the method described can be generalized to other well characterized commercial thermal pastes with comparable thermal conductivity. Through reusability, minimal sample preparation requirements, and relative ease of use, the proposed method bridges significant gaps in the wide-scale adoption of the 3ω method for high-throughput 3ω measurements.

ACKNOWLEDGMENTS

The authors would like to thank Dr. Kenneth Higa (LBL) for providing the custom pressure measurement setup and Drew Liley (LBL) for assistance with the specific heat capacity measurements. This work was supported by the Assistant Secretary for Energy Efficiency and Renewable Energy, Vehicles Technology Office, of the U.S. Department of Energy under Contract No. DEAC02-05CH11231.

AUTHOR DECLARATIONS

Conflict of Interest

The authors have no conflicts to disclose.

Author Contributions

D.C. and R.T. contributed equally to this work.

D.C., Y.Z., S.K., H.P., and R.S.P. formulated the concept. Y.Z. designed the sensor. R.T. and D.C. performed the experiments, data analysis and sensitivity calculations. D.C., R.T., and R.S.P. wrote the manuscript. All authors reviewed and edited the manuscript.

Divya Chalise: Conceptualization (equal); Data curation (equal); Formal analysis (equal); Investigation (equal); Methodology (equal); Supervision (equal); Visualization (equal); Writing – original draft (equal). **Richard Tee**: Data curation (equal); Investigation (equal); Methodology (equal); Validation (equal); Visualization (equal); Writing – original draft (supporting); Writing – review & editing (supporting). **Yuqiang Zeng**: Conceptualization (supporting); Methodology (equal); Supervision (supporting); Writing – review & editing (equal). **Sumanjeet Kaur**: Conceptualization (supporting); Funding acquisition (equal); Methodology (supporting); Project administration (equal); Supervision (supporting); Writing – review & editing (equal). **Himanshu Pokharna**: Conceptualization (equal); Methodology (supporting); Supervision (supporting); Writing – review & editing (supporting). **Ravi S. Prasher**: Conceptualization (equal); Funding acquisition (equal); Investigation (equal); Methodology (equal); Project administration (equal); Supervision (equal); Writing – review & editing (equal).

DATA AVAILABILITY

The data obtained for this study are available from the corresponding author upon request.

REFERENCES

[1] D. G. Cahill, "Thermal conductivity measurement from 30 to 750 K: the 3ω method," Rev. Sci. Instrum. **61**, 802–808 (1990).

[2] D. G. Cahill, M. Katiyar, and J. R. Abelson, "Thermal conductivity of *a*-Si:H thin films," Phys. Rev. B **50**(9), 6077–6081 (1994).

[3] C. Dames and G. Chen, "1ω, 2ω, and 3ω methods for measurements of thermal properties," Rev. Sci. Instrum. **76**(12), 124902 (2005).

[4] S. D. Lubner, S. Kaur, Y. Fu, V. Battaglia, and R. S. Prasher, "Identification and characterization of the dominant thermal resistance in lithium-ion batteries using *operando* 3-omega sensors," J. Appl. Phys. **127**(10), 105104 (2020).

[5] R. Karthik, N. Harish Nagarajan, B. Raja, and P. Damodharan, "Measurement of thermal conductivity of fluids using 3-ω method in a suspended micro wire," J. Eng. Thermophys. **21**(1), 60–68 (2012).

[6] C. Dames, "Measuring the thermal conductivity of thin films: 3 omega and related electrothermal methods," Annu. Rev. Heat Transfer **16**(1), 7–49 (2013).

[7] S. Kommandur, A. Mahdavifar, P. J. Hesketh, and S. Yee, "A microbridge heater for low power gas sensing based on the 3-Omega technique," Sens. Actuators, A **233**, 231–238 (2015).

[8] C. Clausen, T. Pedersen, and A. Bentien, "The 3-omega method for the measurement of fouling thickness, the liquid flow rate, and surface contact," Sensors **17**, 552 (2017).

[9] Y. Zeng, D. Chalise, Y. Fu, V. Battaglia, S. D. Lubner, and R. S. Prasher, "Operando spatial mapping of lithium concentration using thermal-wave sensing," Joule **5**, 2195–2210 (2021).

[10] D. Chalise *et al.*, "Using thermal interface resistance for non-invasive operando mapping of buried interfacial lithium morphology in-solid state batteries," ACS Appl. Mater. Interf. **15**(13), 17344–17352 (2022).

[11] A. Mazloum, J. Kováčik, Š. Emmer, and I. Sevostianov, "Copper–graphite composites: Thermal expansion, thermal and electrical conductivities, and cross-property connections," J. Mater. Sci. **51**(17), 7977–7990 (2016).

[12] H. Prajapati, D. Ravoori, R. L. Woods, and A. Jain, "Measurement of anisotropic thermal conductivity and inter-layer thermal contact resistance in polymer fused deposition modeling (FDM)," Addit. Manuf. **21**, 84–90 (2018).

[13] H. Prajapati, D. Chalise, D. Ravoori, R. M. Taylor, and A. Jain, "Improvement in build-direction thermal conductivity in extrusion-based polymer additive manufacturing through thermal annealing," Addit. Manuf. **26**, 242–249 (2019).

[14] Q. Zheng, S. Kaur, C. Dames, and R. S. Prasher, "Analysis and improvement of the hot disk transient plane source method for low thermal conductivity materials," Int. J. Heat Mass Transfer **151**, 119331 (2020).

[15] M. Li and M. Akoshima, "Appropriate metallic coating for thermal diffusivity measurement of nonopaque materials with laser flash method and its effect," Int. J. Heat Mass Transfer **148**, 119017 (2020).

09 February 2024 17:58:44

Published under an exclusive license by AIP Publishing

[16]D. G. Cahill, "Analysis of heat flow in layered structures for time-domain thermoreflectance," Rev. Sci. Instrum. **75**(12), 5119–5122 (2004).
[17]M. L. Bauer and P. M. Norris, "General bidirectional thermal characterization via the 3ω technique," Rev. Sci. Instrum. **85**(6), 064903 (2014).
[18]L. Tian *et al.*, "Flexible and stretchable 3ω sensors for thermal characterization of human skin," Adv. Funct. Mater. **27**(26), 1701282 (2017).
[19]R. Wyczółkowski, D. Strychalska, and V. Bagdasaryan, "Correlations for the thermal conductivity of selected steel grades as a function of temperature in the range of 0–800 °C," Arch. Thermodyn. **43**(3), 29–45 (2022).

09 February 2024 17:58:44

Published under an exclusive license by AIP Publishing